



An aptamer-based colorimetric Pt(II) assay based on the use of gold nanoparticles and a cationic polymer

Fuming Sang¹ · Jia Liu¹ · Xue Zhang¹ · Jianxin Pan¹

Received: 1 January 2018 / Accepted: 11 April 2018 / Published online: 25 April 2018
© Springer-Verlag GmbH Austria, part of Springer Nature 2018

Abstract

A colorimetric method is described for the determination of Pt(II). It is based on the use of gold nanoparticles (AuNPs) which are known to aggregate in the presence of a cationic polymer such as poly(diallyldimethylammonium chloride) (PDDA). If, however, a mismatched aptamer (AA) electrostatically binds to PDDA, aggregation is prevented. Upon the addition of Pt(II), it will bind to the aptamer and induce the formation of a hairpin structure. Hence, interaction between aptamer and PDDA is suppressed and PDDA will induce the aggregation of the AuNPs. This is accompanied by a color change from red to blue. The effect can be observed with bare eyes and quantified by colorimetry via measurement of the ratio of absorbances at 610 nm and 520 nm. Response is linear in the 0.24–2 μM Pt(II) concentration range, and the detection limit is 58 nM. The assay is completed within 15 min and selective for Pt(II) even in the presence of other metal ions. It was successfully applied to the rapid determination of Pt(II) in spiked soil samples.

Keywords Colorimetric · Aptasensor · Platinum ions · Cationic polymer · AuNPs aggregation

Introduction

Platinum group as noble metals have been honored as “modern industrial vitamins” and are widely used in automotive catalysts, jewelry, chemical industry, petroleum industry catalyst and aerospace industry. In the field of medicine, platinum drugs, such as cisplatin, oxaliplatin and carboplatin are also widely used for the treatment of tumors based on their interaction with cellular DNA, resulting in the formation of different types of adducts, which is the basis of platinum antitumor activity [1–3]. With the wide use of Pt(II) in chemical, biochemical and pharmaceutical fields, more and more platinum metals come into the environment, which have some potential impacts and do harm to human health [4]. Hence, the detection of Pt(II)

is urgently needed for environmental monitoring and human health.

At present, many methods have been used to detect Pt(II) including atomic absorption spectrometry (AAS) [5], capillary electrophoresis (CE) [6, 7], spectrophotometry [8, 9], inductively coupled plasma mass spectrometry (ICP-MS) [10, 11], etc. Although these methods are accurate and sensitive, they usually require large testing instruments, complicated steps and time-consuming analysis, which limit them from being used in the simple, fast and high-throughput detection. Aptamer based Pt(II) assays have been developed due to their low cost, high specificity and considerable binding constant. For instance, Cai et al. developed a chemiluminescent sensing assay based on the coordination between mismatched streptavidin aptamer (MSAA) and Pt(II) [12]. However, FITC-labelled DNA strand was used in this assay to obtain the fluorescence detection signal. Accordingly, developing a rapid, sensitive and highly selective method for the detection of Pt(II) is of great importance.

Colorimetric assays have attracted increasing attention for their simplicity, low cost and no requirement for sophisticated instruments [13–17]. Especially, Gold nanoparticles (AuNPs) are the most commonly used optical sensing nanomaterials, due to their strong surface plasmon resonance (SPR) absorptions in the visible region [18, 19], simple preparation, high

Electronic supplementary material The online version of this article (<https://doi.org/10.1007/s00604-018-2794-6>) contains supplementary material, which is available to authorized users.

✉ Fuming Sang
sangfuming@hitwh.edu.cn

¹ School of Marine Science and Technology, Harbin Institute of Technology, Weihai 264209, People's Republic of China

stability and biocompatibility. The assays based on salt-induced AuNPs aggregation was still frequently impaired by its low sensitivity [20, 21]. Otherwise, PDDA can not only be highly efficiently in causing the aggregation of AuNPs, but also interact with ssDNA via electrostatic attractions [22–25]. Using these properties, we constructed a colorimetric aptamer assay for Pt(II) detection based on PDDA and aptamer-mediated aggregation of AuNPs in this paper. The results illustrated that the assay was rapid, cheap, highly sensitive and selective for Pt(II) detection. Moreover, it was successfully used in the quantitative detection of Pt(II) in soil samples.

Materials and methods

Reagents and materials

Tetrachloroauric acid (HAuCl_4), potassium tetrachloroplatinate(II) (K_2PtCl_4) and trisodiumcitrate dihydrate ($\text{Na}_3\text{C}_6\text{H}_5\text{O}_7 \cdot 2\text{H}_2\text{O}$) were purchased from Sinopharm Chemical Reagent Co, Ltd. (China, www.sangon.com/). Poly dimethyl diallyl ammonium chloride (PDDA) was bought from Aladdin Ltd. (Shanghai, China). $\text{MgSO}_4 \cdot 7\text{H}_2\text{O}$, $\text{Pb}(\text{CH}_3\text{COO})_2 \cdot 3\text{H}_2\text{O}$, $\text{CaCl}_2 \cdot 2\text{H}_2\text{O}$, $\text{MnCl}_2 \cdot 7\text{H}_2\text{O}$, $\text{ZnSO}_4 \cdot 7\text{H}_2\text{O}$, KCl , $\text{CoCl}_2 \cdot 6\text{H}_2\text{O}$, $\text{NiSO}_4 \cdot 6\text{H}_2\text{O}$, $\text{CdCl}_2 \cdot 2.5\text{H}_2\text{O}$ were purchased from Laiyang Fine Chemical Plant (China, www.lyjxhg09.com.pe168.com/). All oligonucleotides were synthesized and purified with HPLC by Sangon Biotechnology Company, Ltd. (China, www.sangon.com/), and the sequences were listed in Table 1. They were dissolved in distilled water and stored at -20°C . All the solutions were prepared using distilled water (18 $\text{M}\Omega \cdot \text{cm}$).

Instrumentation

UV-vis absorption spectra were measured on a TU1810 UV-vis spectrophotometer (Beijing Purkinje General Instrument, Beijing, China). Transmission Electron Microscope (TEM) images were carried out using a JEOL JEM2010 microscope at 200 kV. Dynamic light scattering (DLS) data were collected on a Zetasizer Nano ZS90 instrumentation (Malvern Instruments Ltd., UK).

Table 1 DNA Sequences used in this study

Name	Sequence (5' to 3')
AA	ATAGACCGCTGTGTGACGCAAGACTGTAT
H1	CGCGCTGCGAATTCAGTCTAGGATTCGGC GTGGGTTAAGAATTCGCAGCGCG
ABA	ACCTGGGGGAGTATTGCGGAGGAAGGT

Synthesis and characterization of AuNPs

The AuNPs were synthesized by reducing HAuCl_4 with sodium citrate according to the approach described in the references [26–28]. All glasswares employed in these preparations were cleaned by being soaked in aqua regia (HCl/HNO_3 3:1 v/v), rinsed thoroughly in water, and oven dried prior to use. A 95 mL aqueous solution of HAuCl_4 (0.01 wt%) was added into a conical flask and heated to 120°C under stirring. And then, freshly prepared trisodium citrate solution (1.2 wt%, 5 mL) was added quickly and consistently stirred and heated until the color of the mixture solution changed from light yellow to dark red. After that, the heater was turned off and stirred for another 10 min. Finally, the solution was cooled to room temperature and stored at 4°C for further use. The AuNPs were characterized by UV-vis spectroscopy, DLS and TEM, respectively. The size of AuNPs was about 13 nm.

Analytical procedure for Pt(II)

10 μL of K_2PtCl_4 with varying concentration, AA (10 μM , 0.5 μL) and Mg^{2+} (1 mM, 0.2 μL) were mixed thoroughly and heated at 88°C for 10 min, and slowly cooled down to room temperature for 1 h, then incubated at 37°C for 30 min to form a hairpin structure. After that, 800 nM PDDA was added into the reaction, thoroughly mixed, and incubated for 10 min. Finally, 200 μL AuNPs (4.9 nM) solution were added and followed by ultrapure water to reach a total volume of 500 μL . After incubation for 5 min, the UV-vis absorption spectra of the sample were measured from 400 to 800 nm using a TU1810 UV-vis spectrophotometer. The ratio value (A_{610}/A_{520}) was used to evaluate the aggregation level of AuNPs [29, 30].

Analysis of real samples

To investigate the practical applicability of the colorimetric assay, we applied it to detect Pt(II) in soil samples. The actual sample used was from the Pt(II) polluted soil in wenhua road (Weihai, Shandong, China). For the analysis of the sample, the sample was pretreated to remove the impurities by aqua regia digestion method. Firstly, the collected dust samples were dried at 100°C in the oven for 12 h, which particle size should be less than 60 mesh. 10 g samples were wetted with water, and 40 mL aqua regia were added to digest the samples at 100°C . We transferred the solution into a 150 mL volumetric flask, and then added ultrapure water to the standard mark of volumetric flask. After that, the solution were filtered to remove insoluble residue. To avoid interference from other metal ions, the filtrate was diluted 1000 times (1000 \times) with distilled water and aqueous ammonia was added to adjust pH to 7. Finally, the samples were spiked with different concentrations of Pt(II) for the colorimetric detection.

Results and discussion

Strategy of the colorimetric assay system for Pt(II)

Scheme 1 illustrates the colorimetric assay mechanism for Pt(II) based on the specific reaction among PDDA, AuNPs, Pt(II) and aptamer (AA) with four mismatched guanine bases (Table 1). In the absence of Pt(II), AA hybridize to form a duplex with cationic polymer (PDDA) via electrostatic attraction. Hence, the aggregation of AuNPs is restrained, and AuNPs can retain their red color due to the insufficient PDDA. In the presence of Pt(II), AA can bind with Pt(II) through the two adjacent guanine (G) and its random coil structure is changed to a hairpin structure, which prevents its interaction with PDDA. Accordingly, the obvious change in the color of the AuNPs from red to blue is observed by the bare eyes, accompanied by SPR absorption peaks change in intensity and wavelength (520 nm to 610 nm). Moreover, the color change extent and SPR intensity change of AuNPs correlate with the concentration of Pt(II), which provides a bare eye and spectroscopic assay for the detection of Pt(II).

In order to intuitively explore the feasibility of the colorimetric method strategy, the validated experiments were conducted by TEM, DLS and CD. All the results are shown in Fig. 1 and S1. AuNPs became aggregated due to PDDA-induced aggregation of AuNPs (a blue color, 500 nm, Fig. S1a). However, in the presence of aptamer, AuNPs were well dispersed in solution (a red color, 13 nm, Fig. 1a) due to the interaction between ssDNA and PDDA, resulting the lack of sufficient PDDA to aggregate the AuNPs. On the contrary, it was obviously observed that there was a great increase in the amount of the aggregated AuNPs with the increase of the

Pt(II) concentration, as shown in Fig. 1c and S1c. The aggregation-dominated processes are further authenticated by the DLS data, which are presented in Fig. 1b, d, S1b and d. The average sizes of the AuNPs changed gradually as the increase of the Pt(II) concentration (13, 72 and 116 nm, respectively). DLS Data further authenticate the above processes, which are well consistent with the TEM images.

In order to further confirm the affinity of AA aptamer to Pt(II) and PDDA, circular dichroism (CD) measurement was used to monitor the conformation change of AA aptamer. As shown in Fig. 2, addition of PDDA caused almost no change of the CD spectra of the AA aptamer, which demonstrated that DNA still retained its original conformation [31]. In the presence of Pt(II), the value of the negative and positive peaks (240–250 nm, 270–280 nm) were decreased with the increase of Pt(II) concentration, but the peaks position almost remained unchanged. The results indicated that Pt(II) can bind to AA aptamer and cause its conformation change, which inhibited strong $\pi \rightarrow \pi^*$ transition of bases with ribodesose, thus resulting in the decrease of CD peak [32]. Accordingly, all the aforementioned results further validated the feasibility of the colorimetric assay strategy (as shown in Scheme 1).

Optimization of detection conditions

In order to obtain a highly sensitive colorimetric assay for Pt(II), all the reaction condition including PDDA, aptamer, Mg^{2+} concentration, pH and the incubation time were optimized. Firstly, 40 μ L of PDDA with various concentrations were incubated with 200 μ L AuNPs solution for 15 min. As seen in Fig. S2, as the amount of PDDA rised, the degree of AuNPs aggregation increased. 800 nM PDDA was suitable to

Scheme 1 A scheme depicts the proposed colorimetric aptasensor for the detection of Pt(II). AA: aptamer; PDDA: poly(diallyldimethylammonium chloride); AuNPs: gold nanoparticles

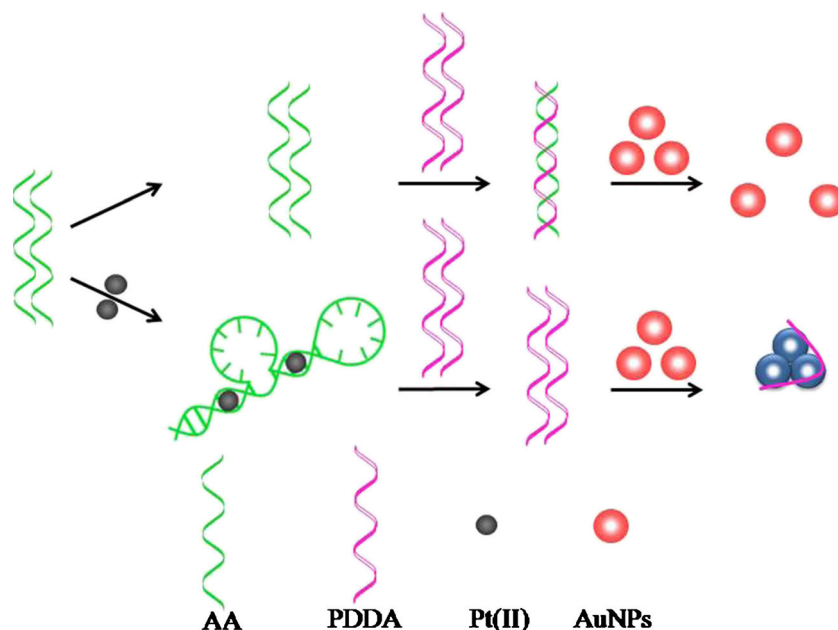
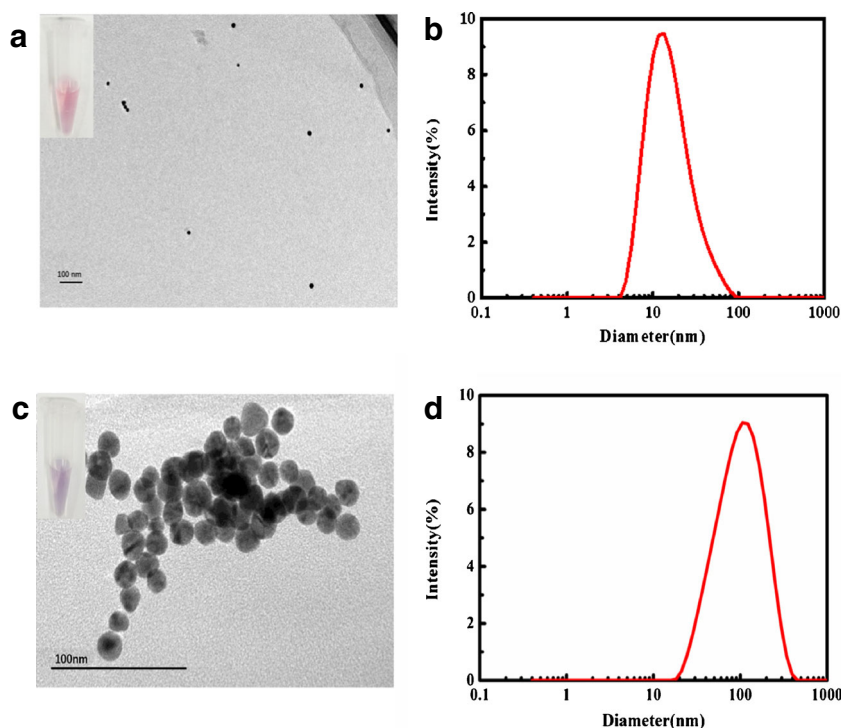


Fig. 1 TEM images of AuNPs treated with different conditions: **a** AuNPs after the treatment with 800 nM PDDA and 8 nM AA; **c** AuNPs after the treatment with 8 nM AA, 2 μ M Pt(II) and 800 nM PDDA; DLS of AuNPs treated with different conditions: **b** AuNPs after the treatment with 800 nM PDDA and 8 nM AA; **d** AuNPs after the treatment with 8 nM AA, 2 μ M Pt(II) and 800 nM PDDA



aggregate all the AuNPs and change the color of AuNPs from red to blue. Moreover, the ratio value of A_{610}/A_{520} attained the maximum and remained almostly unchanged as the concentration reached 800 nM. Hence, 800 nM PDDA was chosen as the optimal concentration in subsequent experiments. Then, the concentration of the aptamer (AA) was optimized at a fixed concentration of 800 nM PDDA, which hybridized with PDDA and keep the red color of AuNPs. Hence, different concentrations of AA (0–14 nM) were firstly incubated with 800 nM PDDA for 10 min, then followed by the addition of

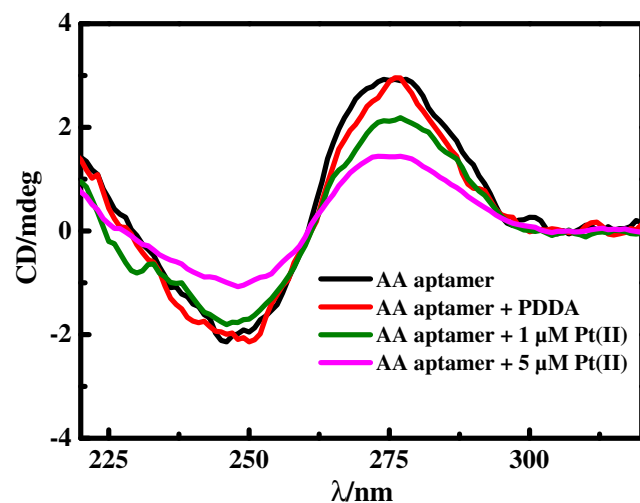


Fig. 2 CD spectra of AA aptamer solution treated with PDDA and Pt(II). Experimental conditions: 700 nM AA aptamer and 800 nM PDDA

AuNPs solution (200 μ L). Figure S3 shows that 8 nM AA can completely prevent the aggregation of AuNPs thereby maintaining the red color of AuNPs, and the minimum A_{610}/A_{520} value is attained. Therefore, 8 nM AA was the optimal concentration and used in the following experiments. The optimal concentration of Mg^{2+} can mediate the binding of aptamer-target [12, 33, 34]. Mg^{2+} promoted the formation of the probe hairpin-like structure. Therefore, varying concentrations of $MgCl_2$ (0, 0.5, 1, 2, 4, 6 mM) were added into the assay system in the absence and presence of Pt(II), respectively. The photographs of AuNPs with different concentrations of $MgCl_2$ are demonstrated in Fig. S4a and b. The great difference in color was observed at 1 mM $MgCl_2$. In addition, the A_{610}/A_{520} value differences between the absence and presence of Pt(II) are shown in Fig. 3. The maximum difference value (0.72) was found when 1 mM $MgCl_2$ was added, which was according to the photographs images. Consequently, 1 mM $MgCl_2$ was applied as the optimal concentration in subsequent experiments. The pH is very important because it affects not only the aggregation of AuNPs but also the color development progress. We firstly investigated the pH effect on AuNPs from 4 to 13, and the results are shown in Fig. S5a. When pH is lower than 4, the dispersed AuNPs aggregated easily themselves. In the range of pH 5–13, the absorption spectra and color of AuNPs solution were almostly unchanged, which illustrated that AuNPs can retain stable over a wide range of pH. Then, we investigated the pH influence on the color development progress in the pH range from 5 to 13. Between pH 5 to 13, the A_{610}/A_{520} value remained unchanged almostly

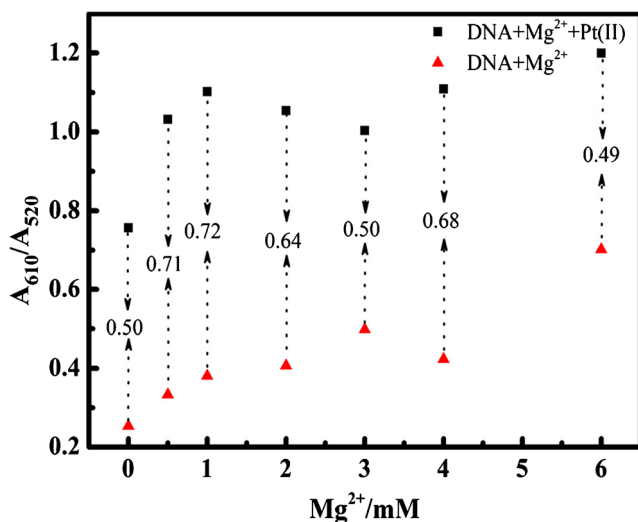


Fig. 3 The effects of Mg²⁺ concentration on the hairpin formation and the ratio values of A₆₁₀/A₅₂₀ of AuNPs in the different concentration of Mg²⁺ (0 to 6 mM). Experimental conditions: 8 nM AA + different concentration of Mg²⁺ + 4 μM Pt(II) + 800 nM PDDA + 200 μL AuNPs

(Fig. S5b). Consequently, pH 7 was used in the all experiments. The incubation time of the Pt(II) with the AA was also investigated and optimized at 37 °C. As shown in Fig. S6, the ratio of A₆₁₀ / A₅₂₀ increased with the increasing of hybridization time, and then remained almost constant after 30 min. Accordingly, 30 min was adopted as the optimal hybridization reaction time.

Colorimetric detection of Pt(II)

Under the optimum reaction conditions, the assay was used to the detection of Pt(II). Different concentrations of Pt(II) solution from 0 to 8 μM were added, and the absorption spectra and the values at 520 and 610 nm were recorded respectively. As shown in Fig. S7, the color of the solution changed gradually from wine red to blue-purple with the increase of Pt(II) concentration, indicating the gradual aggregation of AuNPs. Moreover, the absorbance of AuNPs at 520 nm gradually decreased, and the absorbances of new peak at 610 nm were progressively increased, which were concomitant with the color changes from red to blue-purple. According, the absorption ratio (A₆₁₀/A₅₂₀) was plotted and good linear relationship was attained between the ratio of A₆₁₀/A₅₂₀ and concentrations of Pt(II) with a correlation coefficient of $R^2 = 0.996$ (Fig. 4). In order to further evaluate the sensitivity of the system, $3\alpha/\text{slope}$ was used to calculate the detection limit of the biosensor [20, 25, 32]. The detection limit was 58 nM, which compared favorably with the majority of previous analytical methods, as shown in Table S1. Furthermore, compared with the previously reported detection methods, the method had several advantages. First,

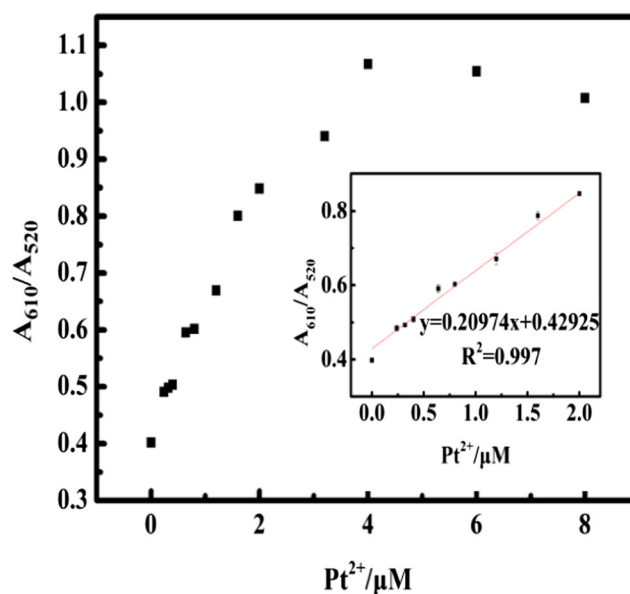


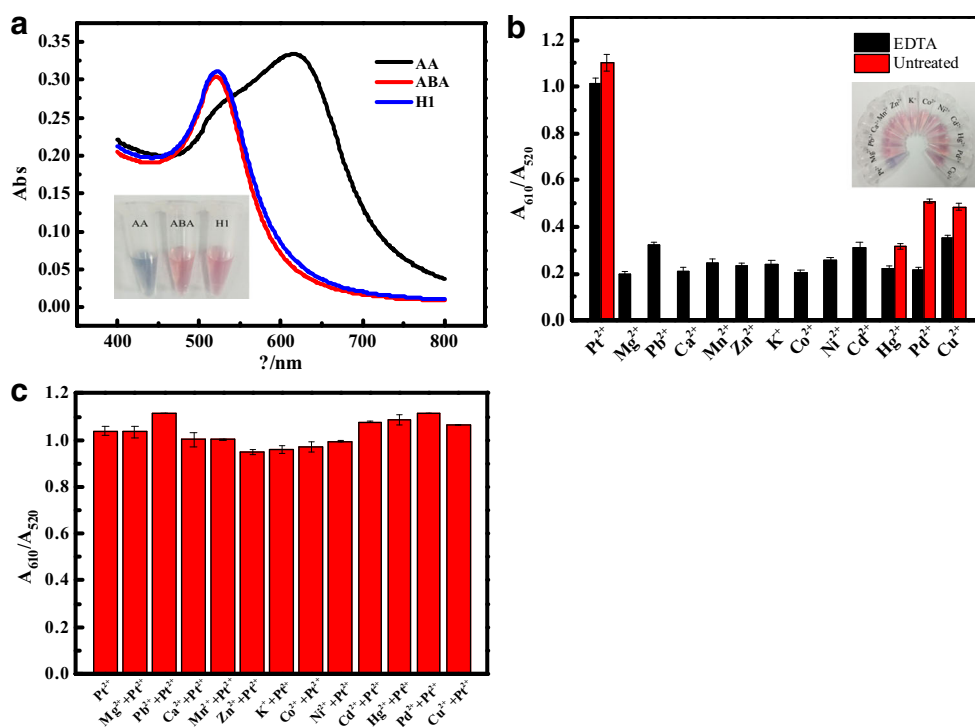
Fig. 4 Sensitivity of the assay for the detection of Pt (II). Plot of A₆₁₀ / A₅₂₀ values versus the concentration of Pt(II) in the range of 0 to 8 μM. The inset shows the linear calibration plot for Pt(II) detection. Error bars were obtained from three experiments. Experimental conditions: 8 nM AA + 1 mM Mg²⁺ + different concentration of Pt(II) + 800 nM PDDA + 200 μL AuNPs

this method did not need expensive apparatus and complicated preparation process and was a simple and cost-effective colorimetric assay. Second, The detection process of Pt(II) can be visualized by the bare eye, and the total detection procedure can be accomplished within just 15 min, which thus give a rapid and sensitive detection of Pt(II).

Selectivity

The selectivity of the biosensor depends on the specific coordination of AA and Pt(II). Therefore, we researched the selectivity of the colorimetric method through two aspects: different DNA sequences and other metal ions. As for the specificity of AA, two random sequences including ABA and H1 (as shown in Table 1) were used. As shown in Fig. 5a, the specific strand visibly rendered AuNPs in the aggregated state with a blue color, which distinctly discriminated from the other two random ones. The UV-vis spectra of the specific strand showed a remarkable red shift compared with the other two random ones. As demonstrated in Fig. S8a, UV-vis spectra of Pt(II) show a striking red shift compared with the other metal ions except for Cu²⁺, Hg²⁺ and Pd²⁺. The results demonstrated that Cu²⁺, Hg²⁺ and Pd²⁺ displayed some influence for Pt(II) detection, due to their interaction with the AA aptamer. To improve the selectivity of the assay, EDTA were chosen for masking the above ions [35],

Fig. 5 Selectivity of the biosensor for the detection of Pt(II). **a** Absorbance spectra of AuNPs in the presence of same concentrations of AA and the other two random sequences (8 nM), 4 μ M Pt(II) was used; **b** The ratio values of A_{610}/A_{520} in the presence of Pt(II) (4 μ M) and other ions (8 μ M), 5 μ M EDTA was used; **c** The ratio values of A_{610}/A_{520} in the presence of Pt(II) (4 μ M) or the mixtures of Pt(II) (4 μ M) and other ions (8 μ M). Experimental conditions: 8 nM AA + 1 mM Mg^{2+} + 4 μ M Pt(II)/ other ions (8 μ M) + 800 nM PDDA + 200 μ L AuNPs. Inset showed the corresponding photos of the solutions



because it had the stability constant ($\log K$) of 18.7 for Cu^{2+} , 18.5 for Pd^{2+} , 21.8 for Hg^{2+} and 16.31 for Pt(II). As shown in Fig. 5b and S8b, the interference from Cu^{2+} , Hg^{2+} and Pd^{2+} has been reduced, whereas the analysis of Pt(II) is almost unaffected in the presence of EDTA ligand. All of the above results illustrated the excellent selectivity for Pt(II) of the colorimetric assay. To further evaluate the selectivity of the biosensor, different interfering ions (8 μ M) were incubated with Pt(II) (4 μ M), respectively. Figure 5c shows the A_{610}/A_{520} value of AuNPs response of the mixture of Pt(II) and other types of ions added as the above, which authenticated that different interfering ions did not affect the assay of Pt(II).

Real sample analysis

In order to explore the practical feasibility of the colorimetric assay, we applied it to detect Pt(II) in real soil samples. The soil samples were spiked with different

Table 2 Determination of spiked Pt (II) in soil sample ($n = 5$)

Sample	ICP-MS (μ M)	This method + SD	Recovery	RSD
0.9 μ M	0.95	0.95 ± 0.043	105.55	4.46
1.5 μ M	1.59	1.54 ± 0.074	102.67	4.80
2.0 μ M	2.12	2.06 ± 0.070	103.0	3.42

concentrations of Pt(II) detected by the colorimetric assay. As shown in Table 2, the recoveries of the spiked Pt(II) samples were in the range of 102.67–105.55% with the RSD less than 3.42–4.80% ($n = 5$). In order to validate the accuracy of our method, these samples were also analysed using the standard ICP-MS method. The data in Table 2 illustrated that our method were in agreement with those of the ICP-MS methods. Therefore, this colorimetric assay had the potential applicability for on-site, rapid and reliable detection of Pt(II) in environment and urine samples without time-consuming and expensive instrumentation analysis. Moreover, the method can hold promising potential for other kinds of Pt(II) drugs detection.

Conclusions

A colorimetric assay is described for simple and rapid detection of Pt(II) based on PDDA and DNA-mediated aggregation of AuNPs. In the optimum condition, the assay demonstrated a low detection limit of low as 58 nM and high selectivity for Pt(II). More importantly, the method has been successfully used in detection of Pt(II) in soil samples. All of the above results illustrated that the method had the great potential for the rapid, sensitive and on-site detection of Pt(II) in the aqueous biological and environmental samples.

Acknowledgments This work was funded by the Natural Science Foundation of China (NSFC) (No. 21407035), Shandong Provincial Natural Science Foundation (ZR2014BM021), Technology and Development Program of Weihai (2014DXGJ15), HIT-NSRIF (2011101).

Compliance with ethical standards We declare that we have no conflict of interest.

References

- Brabec V, Kasparkova J (2005) Modifications of DNA by platinum complexes. Relation to resistance of tumors to platinum antitumor drugs. *Drug Resist Updat* 8(3):131–146
- Oza AM, Cibula D, Benzaquen AO, Poole C, Mathijssen RHJ, Sonke GS, Colombo N, Špaček J, Vuylsteke P, Hirte H (2015) Olaparib combined with chemotherapy for recurrent platinum-sensitive ovarian cancer: a randomised phase 2 trial. *Lancet Oncol* 16(1):87–97
- Orecchio S, Amorello D, Carollo C (2012) Voltammetric determination of platinum in perfusate and blood: preliminary data on pharmacokinetic study of arterial infusion with oxaliplatin. *Microchem J* 100(1):72–76
- Rudolph E, Hann S, Stingeder G, Reiter C (2005) Ultra-trace analysis of platinum in human tissue samples. *Anal Bioanal Chem* 382(7):1500–1506
- Brouwers EE, Tibben MM, Joerger M, Van TO, Rosing H, Schellens JH, Beijnen JH (2005) Determination of oxaliplatin in human plasma and plasma ultrafiltrate by graphite-furnace atomic-absorption spectrometry. *Anal Bioanal Chem* 382(7):1484–1490
- Ip V, Mckeage M, Thompson P, Damianovich D, Findlay M, Liu J (2008) Platinum-specific detection and quantification of oxaliplatin and Pt (R,R-diaminocyclohexane) Cl₂ in the blood plasma of colorectal cancer patients. *J Anal Atom Spectrom* 23(6):881–884
- Fabian M, Solomaha E, Olson JS, Maresso AW (2009) Quantification of cisplatin, carboplatin and oxaliplatin in spiked human plasma samples by ICP-SFMS and hydrophilic interaction liquid chromatography (HILIC) combined with ICP-MS detection. *J Anal Atom Spectrom* 24(10):1336–1342
- Huang Z, Timerbaev AR, Keppler BK, Hirokawa T (2006) Determination of cisplatin and its hydrolytic metabolite in human serum by capillary electrophoresis techniques. *J Chromatogr A* 1106(1–2):75–79
- Yang H, Cui H, Wang L, Yan L, Qian Y, Zheng XE, Wei W, Zhao J (2014) A label-free G-quadruplex DNA-based fluorescence method for highly sensitive, direct detection of cisplatin. *Assay Actuat B Chem* 202(10):714–720
- Martinčić A, Cemazar M, Sersa G, Kovač V, Milačić R, Ščančar J (2013) A novel method for speciation of Pt in human serum incubated with cisplatin, oxaliplatin and carboplatin by conjoint liquid chromatography on monolithic disks with UV and ICP-MS detection. *Talanta* 116(22):141–148
- Yaroshenko DV, Grigoriev AV, Sidorova AA, Kartsova LA (2013) Determination of cisplatin in blood plasma by liquid chromatography with mass spectrometry detection. *J Anal Chem* 68(2):156–160
- Cai S, Tian X, Sun L, Hu H, Zheng S, Jiang H, Yu L, Zeng S (2015) Platinum (II)-oligonucleotide coordination based aptasensor for simple and selective detection of platinum compounds. *Anal Chem* 87(20):10542–10546
- Niu S, Lv Z, Liu J, Bai W, Yang S, Chen A (2014) Colorimetric aptasensor using unmodified gold nanoparticles for homogeneous multiplex detection. *PLoS One* 9(10):e109263
- Sang F, Li X, Zhang Z, Liu J, Chen G (2017) Recyclable colorimetric sensor of Cr³⁺ and Pb²⁺ ions simultaneously using a zwitterionic amino acid modified gold nanoparticles. *Spectrochim Part A* 193:109–116
- Zhang Y, Li R, Xue Q, Li H, Liu J (2015) Colorimetric determination of copper(II) using a polyamine-functionalized gold nanoparticle probe. *Microchim Acta* 182(9–10):1677–1683
- He Y, Cheng F, Pang DW, Tang HW (2016) Colorimetric and visual determination of DNase I activity using gold nanoparticles as an indicator. *Microchim Acta* 184(1):1–6
- Du G, Zhang D, Xia B, Xu L, Wu S, Zhan S, Ni X, Zhou X, Wang L (2016) A label-free colorimetric progesterone aptasensor based on the aggregation of gold nanoparticles. *Microchim Acta* 183(7):2251–2258
- Li J, Tu W, Li H, Han M, Lan Y, Dai Z, Bao J (2014) In situ-generated nano-gold plasmon-enhanced photoelectrochemical aptasensing based on carboxylated perylene-functionalized graphene. *Anal Chem* 86(2):1306–1312
- Liu S, Du Z, Li P, Li F (2012) Sensitive colorimetric visualization of dihydronicotinamide adenine dinucleotide based on anti-aggregation of gold nanoparticles via boronic acid-diol binding. *Biosens Bioelectron* 35(1):443–446
- Fan D, Zhai Q, Zhou W, Zhu X, Wang E, Dong S (2016) A label-free colorimetric aptasensor for simple, sensitive and selective detection of Pt (II) based on platinum (II)-oligonucleotide coordination induced gold nanoparticles aggregation. *Biosens Bioelectron* 85:771–776
- Pires TA, Narovec CM, Whelan RJ (2017) Effects of cationic proteins on gold nanoparticle/aptamer assays. *ACS Omega* 2(11):8222–8226
- Chen Z, Tan Y, Zhang C, Yin L, Ma H, Ye N, Qiang H, Lin Y (2014) A colorimetric aptamer biosensor based on cationic polymer and gold nanoparticles for the ultrasensitive detection of thrombin. *Biosens Bioelectron* 56(1):46–50
- Jeon W, Lee S, Manjunatha DH, Ban C (2013) A colorimetric aptasensor for the diagnosis of malaria based on cationic polymers and gold nanoparticles. *Anal Biochem* 439:6–11
- Luan Y, Chen J, Li C, Xie G, Fu H, Ma Z, Lu A (2015) Highly sensitive colorimetric detection of ochratoxin A by a label-free aptamer and gold nanoparticles. *Toxins* 7(12):5377–5385
- Bala R, Kumar M, Bansal K, Sharma RK, Wangoo N (2016) Ultrasensitive aptamer biosensor for malathion detection based on cationic polymer and gold nanoparticles. *Biosens Bioelectron* 85:445–449
- Turkevich J, Stevenson PC, Hillier J (1951) A study of the nucleation and growth processes in the synthesis of colloidal gold. *Discuss Faraday Soc* 11(11):55–75
- Ji XH, Song XN, Li J, Bai YB, Yang WS, Peng XG (2007) Size control of gold nanocrystals in citrate reduction: the third role of citrate. *J Am Chem Soc* 129(45):13939–13948
- Sanfelice RC, Pavinatto A, Gonçalves VC, Correa DS, Mattoso LHC, Balogh DT (2016) Synthesis of a nanocomposite containing a water-soluble polythiophene derivative and gold nanoparticles. *J Polym Sci Pol Phys* 54(13):1245–1254
- Zhan S, Yu M, Lv J, Wang L, Zhou P (2014) Colorimetric detection of trace arsenic (III) in aqueous solution using arsenic aptamer and gold nanoparticles. *Aust J Chem* 67(5):813–818
- Wu Y, Liu L, Zhan S, Wang F, Zhou P (2012) Ultrasensitive aptamer biosensor for arsenic (III) detection in aqueous solution based on surfactant-induced aggregation of gold nanoparticles. *Analyst* 137(18):4171–4178
- Zhang D, Yang J, Ye J, Xu L, Xu H, Zhan S, Xia B, Wang L (2016) Colorimetric detection of bisphenol A based on unmodified aptamer and cationic polymer aggregated gold nanoparticles. *Anal Biochem* 499:51–56

32. Wu Y, Zhan S, Wang L, Zhou P (2014) Selection of a DNA aptamer for cadmium detection based on cationic polymer mediated aggregation of gold nanoparticles. *Analyst* 139(6):1550–1561
33. Tan L, Chen Z, Zhang C, Wei X, Lou T, Zhao Y (2017) Colorimetric detection of Hg^{2+} based on the growth of aptamer-coated AuNPs: the effect of prolonging aptamer strands. *Small* 13(14):1–8
34. Owczarzy R, Moreira BG, You Y, Behlke MA, Walder JA (2008) Predicting stability of DNA duplexes in solutions containing magnesium and monovalent cations. *Biochemist* 47(19):5336–5353
35. Zhang M, Liu YQ, Ye BC (2012) Colorimetric assay for parallel detection of Cd^{2+} , Ni^{2+} and Co^{2+} using peptide-modified gold nanoparticles. *Analyst* 137(3):601–607